# Lepton flavor violation in photon-induced electron-muon pairs at the HL-LHC

M. A. Arroyo-Ureña, 1, 2, \* O. Félix-Beltrán, 3, † J. Hernández-Sánchez, 3, ‡ C. G. Honorato, 3, § and S. Rosado-Navarro<sup>4</sup>, ¶

<sup>1</sup>Facultad de Ciencias Físico-Matemáticas

 <sup>2</sup> Centro Interdisciplinario de Investigación y Enseñanza de la Ciencia (CHEC), Benemérita Universidad Autónoma de Puebla, C.P. 72570, Puebla, Pue., México,
 <sup>3</sup> Facultad de Ciencias de la Electrónica, Benemérita Universidad Autónoma de Puebla, Apartado Postal 1152, C.P. 72570, Puebla, Pue., México.
 <sup>4</sup> Centro Interdisciplinario de Investigación y Enseñanza de la Ciencia (CHEC), Benemérita Universidad Autónoma de Puebla, C.P. 72570, Puebla, México.

We show the outstanding potential of the High-Luminosity LHC (HL-LHC) to discover charged lepton flavor violation (cLFV) via the ultra-peripheral process  $\gamma\gamma\to e^\pm\mu^\mp$ . Using a gauge-invariant Effective Field Theory (EFT) framework—consistent with the most stringent bounds from radiative decays—we perform a full Monte Carlo analysis with multivariate techniques. Our results show that a  $5\sigma$  discovery is achievable with an integrated luminosity of  $\mathcal{L}_{\rm int}\gtrsim 2700~{\rm fb}^{-1}$  for favorable benchmark scenarios. This study establishes photon-fusion at the HL-LHC as a powerful probe of cLFV, strongly motivating dedicated searches by the experimental collaborations.

# I. INTRODUCTION

In the Standard Model (SM), LFV is strictly forbidden. However, the observation of neutrino oscillations has confirmed that such particles have non-zero masses, which introduces LFV in the neutral sector. Within the SM framework, cLFV processes remain highly suppressed due to the GIM mechanism. Consequently, any experimental observation of a cLFV process would constitute unambiguous evidence for physics beyond the SM (BSM). In this work, we aim to explore the  $\gamma\gamma e\mu$  interaction within an EFT framework and assess its prospects for experimental scrutiny at the HL-LHC [1]. An analogous method, but in  $e^-e^+$  colliders, is studied in [2]. This strategy leverages photon-photon interactions in ultraperipheral collisions (UPCs), where these type of interactions provide a pristine environment for studying electromagnetic phenomena, as they are precisely described by Quantum Electrodynamics (QED), and can be efficiently modeled using the equivalent photon approximation (EPA).

A confrontation of the EFT predictions against current experimental bounds, shows that the most stringent constraint on the diphoton operators originates from the loop-induced radiative decays  $\mu \to e \gamma$  [3]. However, even after accommodating this constraint by suppressing the relevant theory parameters, a viable region of parameter space is found, providing strong motivation for experimental searches.

# II. THEORETICAL FRAMEWORK

The local cLFV  $\gamma\gamma\ell_i\ell_j$  interaction is described by the effective Lagrangian [4]:

$$\mathcal{L}_{\text{eff}} = \left( G_{SR}^{ij} \bar{\ell}_{L_i} \ell_{R_j} + G_{SL}^{ij} \bar{\ell}_{R_i} \ell_{L_j} \right) F_{\mu\nu} F^{\mu\nu} + \left( \tilde{G}_{SR}^{ij} \bar{\ell}_{L_i} \ell_{R_j} + \tilde{G}_{SL}^{ij} \bar{\ell}_{R_i} \ell_{L_j} \right) \tilde{F}_{\mu\nu} F^{\mu\nu} + \text{H.c.}, \quad (1)$$

where  $\ell_i$ ,  $\ell_j = e$ ,  $\mu$ ,  $\tau$  denote the lepton flavors,  $F_{\mu\nu}$  is the electromagnetic field strength tensor, and  $\tilde{F}_{\mu\nu} = \frac{1}{2}\epsilon_{\mu\nu\sigma\lambda}F^{\sigma\lambda}$  is its dual. The couplings  $G_{SR}^{ij}$ ,  $G_{SL}^{ij}$ ,  $\tilde{G}_{SR}^{ij}$ , and  $\tilde{G}_{SL}^{ij}$  are dimensionful, scaling as  $\Lambda^{-3}$ , where  $\Lambda$  is the energy cutoff of the EFT. This scaling is characteristic of dimension-7 operators in an EFT extension of the SM, where LFV processes are forbidden at tree level but can be induced in scenarios BSM.

The free effective coupling that has a direct impact on the process  $\gamma\gamma e\mu$  is controlled by  $|G_{e\mu}|$ . This effective coupling encapsulates the relevant operator coefficients, and can be written as:

$$|G_{e\mu}|^2 = 2(|G_P^{e\mu}|^2 + |G_S^{e\mu}|^2 + |\tilde{G}_P^{e\mu}|^2 + |\tilde{G}_S^{e\mu}|^2),$$
 (2)

where

$$G_{S}^{e\mu} = \frac{G_{SR}^{e\mu} + G_{SL}^{e\mu}}{2}, \quad G_{P}^{e\mu} = \frac{G_{SR}^{e\mu} - G_{SL}^{e\mu}}{2},$$
$$\tilde{G}_{S}^{e\mu} = \frac{\tilde{G}_{SR}^{e\mu} + \tilde{G}_{SL}^{e\mu}}{2}, \quad \tilde{G}_{P}^{e\mu} = \frac{\tilde{G}_{SR}^{e\mu} - \tilde{G}_{SL}^{e\mu}}{2}. \quad (3)$$

From the upper limit on BR( $\mu \to e\gamma$ ), a stringent constraint on the effective coupling  $|G_{e\mu}|$  is found [5]:

$$|G_{\mu e}| \lesssim 1.2 \times 10^{-10} \left( 1 + 0.15 \ln \frac{\Lambda}{100 \text{ GeV}} \right)^{-1} \text{ GeV}^{-3}.$$
(4)

From Eqs. (4) and (2), we obtain the parameter space

<sup>\*</sup> marco.arroyo@fcfm.buap.mx

 $<sup>^{\</sup>dagger}$ olga.felix@correo.buap.mx

<sup>&</sup>lt;sup>‡</sup> jaime.hernandez@correo.buap.mx

<sup>§</sup> carlosg.honorato@correo.buap.mx

 $<sup>\</sup>P$  sebastian.rosado@protonmail.com

presented in Fig. 1.

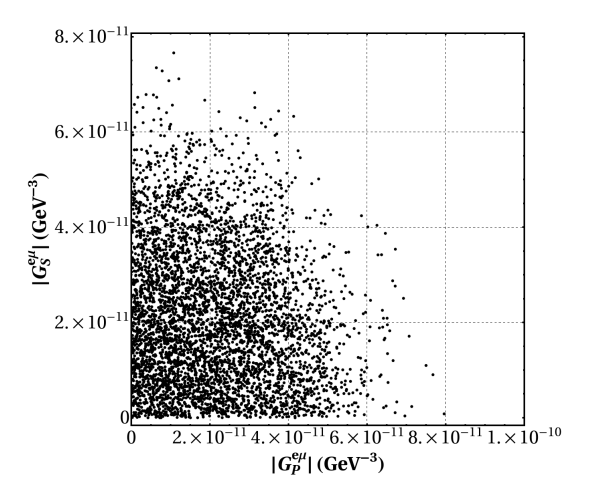


FIG. 1: Parameter space in the  $|G_S^{e\mu}| - |G_P^{e\mu}|$ . We scan the intervals  $|G_{S,P}^{e\mu}|$ ,  $|\tilde{G}_{S,P}^{e\mu}| \in [0,10^{-9}] \text{ GeV}^{-3}$  and  $\Lambda \in (100, 5000) \text{ GeV}$ . The black points represent those allowed by the constraints in Eqs. (4) and (2).

For this study, we select the benchmark values of the cut-off scale such as  $\Lambda \gg \sqrt{s_{\gamma\gamma}}$ , where  $\sqrt{s_{\gamma\gamma}}$  is the centerof-mass energy of the  $\gamma\gamma$  system . This choice is motivated by the requirement that the EFT expansion remains consistent; specifically, for  $\Lambda \gtrsim 2\sqrt{s_{\gamma\gamma}}$ , contributions from a dimension-d operator are suppressed by at least  $(\sqrt{s_{\gamma\gamma}}/\Lambda)^{d-4}$ , ensuring non-renormalizable terms remain under control. The center-of-mass energy required to produce an  $e\mu$  pair is  $\sqrt{s_{\gamma\gamma}} \gtrsim m_{\mu}$ , which might naively suggest that a low effective scale  $\Lambda$  could suffice. However, values of  $\Lambda \lesssim 100$  GeV are incompatible with the EFT framework, as they would invalidate its core assumption that  $\Lambda$  is significantly larger than the energy scale of the process. In fact, such a low  $\Lambda$  would imply the existence of new particles with masses near or below the electroweak scale, which would require their explicit inclusion in the SM rather than a description through effective operators.

Accordingly, we will explore three BP's to span the viable parameter space:

• **BP1**:  $\Lambda = 1048 \, \text{GeV}$ ,

$$\begin{split} |G_S^{e\mu}| &= 3.85 \times 10^{-11} \, \mathrm{GeV}^{-3}, \, |G_P^{e\mu}| = 4.25 \times 10^{-11} \, \mathrm{GeV}^{-3}, \\ |\tilde{G}_S^{e\mu}| &= 1.91 \times 10^{-12} \, \mathrm{GeV}^{-3}, \, |\tilde{G}_P^{e\mu}| = 2.42 \times 10^{-12} \, \mathrm{GeV}^{-3}, \end{split}$$

• **BP2**:  $\Lambda = 730 \,\text{GeV}$ ,

$$\begin{split} |G_S^{e\mu}| &= 5.22 \times 10^{-11} \, \mathrm{GeV^{-3}}, \, |G_P^{e\mu}| = 1.46 \times 10^{-11} \, \mathrm{GeV^{-3}}, \\ |\tilde{G}_S^{e\mu}| &= 2.47 \times 10^{-11} \, \mathrm{GeV^{-3}}, \, |\tilde{G}_P^{e\mu}| = 5.96 \times 10^{-12} \, \mathrm{GeV^{-3}}, \end{split}$$

• **BP3**:  $\Lambda = 1859 \, \text{GeV}$ ,

$$\begin{split} |G_S^{e\mu}| &= 2.70 \times 10^{-11} \, \mathrm{GeV^{-3}}, \, |G_P^{e\mu}| = 1.92 \times 10^{-11} \, \mathrm{GeV^{-3}}, \\ |\tilde{G}_S^{e\mu}| &= 3.26 \times 10^{-11} \, \mathrm{GeV^{-3}}, \, |\tilde{G}_P^{e\mu}| = 3.16 \times 10^{-11} \, \mathrm{GeV^{-3}}. \end{split}$$

In addition to these values strictly satisfying stringent current experimental limits, the chosen cutoff scales ( $\Lambda \sim 1-2 \text{ TeV}$ ) are phenomenologically motivated, as they are consistent with interpreting the reported excesses near 95, 150, and 650 GeV as new physics resonances [6, 7]. If one estimates  $M_{\phi_k} \sim C_{e\mu}^k |G_{e\mu}| \Lambda^4$  (k=1,2,3), for our benchmarks, this connection requires coefficients  $C_{e\mu}^k$  of  $\mathcal{O}(1)$ , suggesting a potential common UV origin that our cLFV search uniquely probes<sup>1</sup>.

## III. COLLIDER ANALYSIS

#### A. Signal and background

- **Signal:** We are interested in searching for the final state of an opposite-sign  $e\mu$  pair, which is produced via UPCs  $(\gamma\gamma \to e\mu)$  in proton-proton (pp) collisions.
- Background: The dominant SM backgrounds are  $qq oup W^-W^+$ ,  $\gamma\gamma oup W^+W^-$ , and  $\gamma\gamma oup \tau^-\tau^+ oup e\mu + \nu's$ , with smaller contributions from misidentified hadronic processes. To mitigate the substantial background from pile-up, we employ the delphes\_card\_HLLHC-Pile-up.tcl² configuration. Our simulation includes pile-up with an average of 140 interactions per crossing, corresponding to HL-LHC conditions, via the PileUpMerger module and the pileup per particle identification (PUPPI) algorithm. The sensitivity could be further improved beyond our conservative estimates by using forward proton spectrometers (roman pots) to tag exclusive events and suppress pile-up backgrounds [8, 9].

TABLE I: Production cross sections of the signal for the three BP's. The number of events is evaluated for  $\mathcal{L}_{\text{int}} = 3 \text{ ab}^{-1}$ .

BP's	$\sigma(\gamma\gamma \to e\mu)(\text{fb})$	Events
BP1	0.04	120
BP2	0.035	105
BP3	0.013	39

 $<sup>^1</sup>$  Given that  $|G_{e\mu}|$  has dimensions of GeV  $^{-3},$  the mass  $M_{\phi_k}$  have dimensions of GeV.

 $<sup>^2</sup>$  This card is made available upon request.

The numerical cross sections for the signal and dominant background processes are presented in Tables I and II, respectively. These results incorporate the fiducial cuts  $p_{\tau}^{(e,\,\mu)} > 10$  GeV,  $|\eta^{(e,\,\mu)}| < 2.5$ ,  $\Delta R(e\mu) > 0.4$ .

Signal and background events are generated with MadGraph5 (LanHEP/UFO) -using the electric dipole form factor (EDFF) to model UPC's-, showered with Pythia8, and passed through Delphes3 [10-16].

## B. Multivariate Analysis

The kinematic analysis revealed that the individual observables had relatively weak discriminating power to separate the signal from background. To enhance the selection efficacy, we therefore employed a Multivariate Analysis (MVA) approach, which combines these observables into a single, more powerful discriminant. We use a Boosted Decision Tree (BDT) method [17] based on the XGBoost library's gradient boosting implementation. The BDT classifiers were trained on a set of kinematic variables associated to the final-state objects, including the transverse momentum  $(p_T)$ , pseudorapidity  $(\eta)$ , angular separation  $(\Delta R)$ , transverse and invariant masses  $(M_T, M_{\rm inv})$ , azimutal angle  $(\phi)$ .

The BDT selection is optimized to maximize the figure of merit, *i.e.*, the *signal significance*, defined as  $S = N_S / \sqrt{N_S + N_B + (\kappa \cdot N_B)^2}$  [18], where  $N_S$  and  $N_B$  are the number of signal and background candidates, respectively. The factor  $\kappa = 5\%$  stands for a realistic systematic uncertainty [19].

Building upon the previous MVA, the most powerful discriminating observables for distinguishing the signal from background processes are: i) the angular separation between the electron and muon  $\Delta R(e\mu)$ , ii) transverse mass of the electron  $M_T(e) = \sqrt{2p_T^e E_T(1-\cos\phi_{eE_T})}$ , and iii) missing energy transverse  $E_T$ . The distribution of the most significant variable, which exhibit a pronounced separation between the signal and the several background channels, is presented in Fig. 2.

On the other hand, the absence of over-training is confirmed by a Kolmogorov-Smirnov (KS) test, which yields high scores of 0.49 for background and 0.34 for signal.

The exceptional discovery potential of the signal at the HL-LHC is demonstrated by our key results in Fig. 3, which show the projected signal significance as a function of integrated luminosity and the corresponding BDT

TABLE II: Production cross sections of relevant SM background processes. The number of events is evaluated for  $\mathcal{L}_{int} = 3 \text{ ab}^{-1}$ .

Process	cross section (fb)	Events
$\gamma \gamma \to WW \to e \nu_e \mu \nu_\mu$	0.623	1869
$\gamma \gamma \to \tau \tau \to e \nu_e \nu_\tau \mu \nu_\mu \nu_\tau$	28.2	84600
$qq \to WW \to e\nu_e\mu\nu_\mu$	890	$2.67 \times 10^{6}$

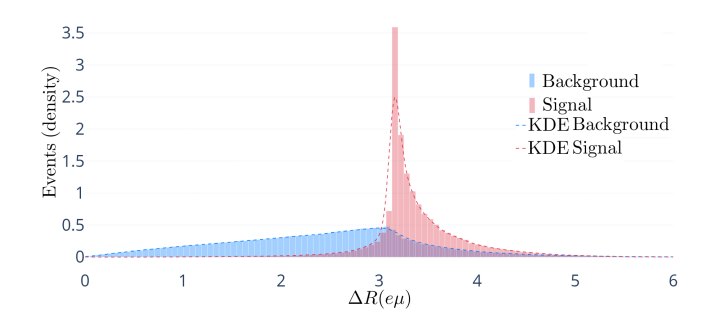


FIG. 2: Angular separation  $\Delta R(e\mu)$ . We also include the fit Kernel Density Estimation (KDE).

classifier outputs for BP1.

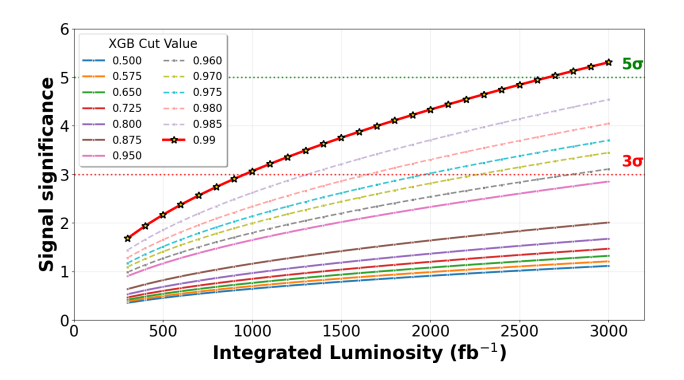


FIG. 3: Signal significance as a function of integrated luminosity and the cut on the BDT prediction for BP1. Systematic uncertainties ( $\kappa = 5\%$ ) are also considered.

The optimal scenario corresponds to BP1, we obtain a signal significance of  $5\sigma$  for  $\mathcal{L}_{\rm int} \gtrsim 2700\,{\rm fb}^{-1}$  and a BDT cut of 0.99. Similar predictions are found for BP2, which predicts that a  $5\sigma$  significance is achievable with  $\mathcal{L}_{\rm int} \gtrsim 2800\,{\rm fb}^{-1}$ . BP3 predicts up to approximately  $2\sigma$  for an integrated luminosity of  $\mathcal{L}_{\rm int} \approx 3000\,{\rm fb}^{-1}$ .

## IV. CONCLUSIONS

We have shown the unique capability of the HL-LHC to probe charged lepton flavor violation through the ultraperipheral process  $pp \to p(\gamma\gamma)p \to p(e^{\pm}\mu^{\mp})p$ . Our analysis, based on a dimension-7 effective field theory framework, reveals a direct connection between the experimental sensitivity and the underlying new physics scale  $\Lambda$ . Crucially, the benchmark points BP1 ( $\Lambda=1048~{\rm GeV}$ ), BP2 ( $\Lambda=730~{\rm GeV}$ ), and BP3 ( $\Lambda=1859~{\rm GeV}$ ) span a phenomenologically meaningful range of cutoff scales. The fact that BP2—with the lowest allowed  $\Lambda$ -yields a strong signal highlights how this channel is particularly sensitive to new physics at the TeV scale. Meanwhile, BP3 demonstrates the challenge of probing higher scales, still remains accessible at high luminosities. Notably, a  $5\sigma$  discovery is achievable for  $\Lambda\sim 1~{\rm TeV}$  with  $\mathcal{L}_{\rm int}\gtrsim 2700$ 

fb<sup>-1</sup>, while scales up to  $\Lambda \sim 2$  TeV may be probed at the approximately  $2\sigma$  level with  $\mathcal{L}_{\rm int} \approx 3000~{\rm fb^{-1}}$ . This clear correlation between the cutoff scale and the required luminosity provides valuable guidance for future searches.

These results strongly motivate dedicated experimental efforts to search for  $\gamma\gamma \to e\mu$  in early HL-LHC data. Future colliders with higher energy reach will be essential to extend this probe to even higher scales, offering a powerful tool to explore lepton flavor violation beyond the TeV frontier [20, 21].

The high photon fluxes in Pb-Pb collisions offer a distinct advantage: they can substantially enhance the production cross section. This enhancement compensates for the lower integrated luminosity, making it a highly

promising channel. The net effect is an estimated increase in the number of observable events by approximately an order of magnitude compared to pp collisions [22, 23].

## ACKNOWLEDGMENTS

We are grateful to Fabiola Fortuna for her invaluable comments. This work was supported by the Estancias Posdoctorales por México program, the Sistema Nacional de Investigadores e Investigadoras (SNII), VIEP-BUAP, and PRODEP (México), and the SECIHTI project No. CBF-2025-G-1187.

- CERN, High-luminosity lhc, https://home.cern/ science/accelerators/high-luminosity-lhc (2024), accessed: 2024-05-16.
- [2] M. A. Arroyo-Ureña, R. Gaitán, M. Marín, H. Salazar, and M. G. Villanueva-Utrilla, Searching for the LFV  $\gamma\gamma e\mu$  interaction at  $e^-e^+$  colliders, (2025), arXiv:2504.12431 [hep-ph].
- [3] A. M. Baldini et al. (MEG), Search for the lepton flavour violating decay  $\mu^+ \to e^+ \gamma$  with the full dataset of the MEG experiment, Eur. Phys. J. C **76**, 434 (2016), arXiv:1605.05081 [hep-ex].
- [4] J. D. Bowman, T. P. Cheng, L.-F. Li, and H. S. Matis, New Upper Limit for  $\mu \to e\gamma\gamma$ , Phys. Rev. Lett. **41**, 442 (1978).
- [5] F. Fortuna, X. Marcano, M. Marín, and P. Roig, Lepton flavor violation from diphoton effective interactions, Phys. Rev. D 108, 015008 (2023), arXiv:2305.04974 [hep-ph].
- [6] S. Bhattacharya, B. Lieberman, M. Kumar, A. Crivellin, Y. Fang, R. Mazini, and B. Mellado, Emerging Excess Consistent with a Narrow Resonance at 152 GeV in High-Energy Proton-Proton Collisions, (2025), arXiv:2503.16245 [hep-ph].
- [7] A. Tumasyan et al. (CMS), Search for a new resonance decaying into two spin-0 bosons in a final state with two photons and two bottom quarks in proton-proton collisions at  $\sqrt{s} = 13$  TeV, JHEP 05, 316, arXiv:2310.01643 [hep-ex].
- [8] G. Aad et al. (ATLAS), Performance of the ATLAS forward proton Time-of-Flight detector in Run 2, JINST 19 (05), P05054, arXiv:2402.06438 [physics.ins-det].
- [9] A. Hayrapetyan et al. (CMS), Observation of  $\gamma\gamma \to \tau\tau$  in proton-proton collisions and limits on the anomalous electromagnetic moments of the  $\tau$  lepton, Rept. Prog. Phys. 87, 107801 (2024), arXiv:2406.03975 [hep-ex].
- [10] A. Semenov, LanHEP A package for automatic generation of Feynman rules from the Lagrangian. Version 3.2, Comput. Phys. Commun. 201, 167 (2016), arXiv:1412.5016 [physics.comp-ph].
- [11] C. Degrande, C. Duhr, B. Fuks, D. Grellscheid, O. Mattelaer, and T. Reiter, UFO The Universal FeynRules Output, Comput. Phys. Commun. 183, 1201 (2012), arXiv:1108.2040 [hep-ph].
- [12] J. Alwall, M. Herquet, F. Maltoni, O. Mattelaer, and T. Stelzer, Madgraph 5: going beyond, Journal of High

- Energy Physics **2011**, 10.1007/jhep06(2011)128 (2011).
- [13] T. Sjöstrand, S. Ask, J. R. Christiansen, R. Corke, N. Desai, P. Ilten, S. Mrenna, S. Prestel, C. O. Rasmussen, and P. Z. Skands, An introduction to PYTHIA 8.2, Comput. Phys. Commun. 191, 159 (2015), arXiv:1410.3012 [hep-ph].
- [14] J. de Favereau, C. Delaere, P. Demin, A. Giammanco, V. Lemaître, A. Mertens, and M. Selvaggi (DELPHES 3), DELPHES 3, A modular framework for fast simulation of a generic collider experiment, JHEP 02, 057, arXiv:1307.6346 [hep-ex].
- [15] D. Collaboration, gitHub repository: https://github.com/delphes/delphes.
- [16] H.-S. Shao and D. d'Enterria, gamma-UPC: automated generation of exclusive photon-photon processes in ultraperipheral proton and nuclear collisions with varying form factors, JHEP 09, 248, arXiv:2207.03012 [hep-ph].
- [17] Y. Coadou, Boosted decision trees 10.1142/9789811234033\_0002 (2022), arXiv:2206.09645 [physics.data-an].
- [18] G. Cowan, Statistics, in Handbook of Particle Detection and Imaging, edited by I. Fleck, M. Titov, C. Grupen, and I. Buvat (Springer International Publishing, Cham, 2021) pp. 117–143.
- [19] Sensitivity to exclusive WW production in photon scattering at the High Luminosity LHC, (2021).
- [20] M. Cepeda et al., Report from Working Group 2: Higgs Physics at the HL-LHC and HE-LHC, CERN Yellow Rep. Monogr. 7, 221 (2019), arXiv:1902.00134 [hep-ph].
- [21] N. Arkani-Hamed, T. Han, M. Mangano, and L.-T. Wang, Physics opportunities of a 100 TeV proton-proton collider, Phys. Rept. 652, 1 (2016), arXiv:1511.06495 [hep-ph].
- [22] M. Klusek-Gawenda, V. P. Goncalves, and A. Szczurek, Light-by-Light scattering in ultraperipheral heavy ion collisions: Estimating inelastic contributions, Phys. Lett. B 867, 139614 (2025), arXiv:2503.08624 [hep-ph].
- [23] D. D'Enterria, D. Martins, and P. Rebello Teles, Two-photon fusion Higgs production in collisions with proton and ion beams at the LHC, HE-LHC, and FCC, Frascati Phys. Ser. 69, 156 (2019).